Am J Physiol Gastrointest Liver Physiol 291: G117–G127, 2006.
First published March 24, 2006; doi:10.1152/ajpgi.00397.2005.

Geldanamycin prevents hemorrhage-induced ATP loss by overexpressing inducible HSP70 and activating pyruvate dehydrogenase

Juliann G. Kiang,[1,2,3] Phillip D. Bowman,[4] Xinyue Lu,[1,3] Yansong Li,[1] Xuan Z. Ding,[1] Baiteng Zhao,[4] Yuang-Taung Juang,[1] James L. Atkins,[1] and George C. Tsokos[1,2]

[1]*Walter Reed Army Institute of Research, Silver Spring; Departments of* [2]*Medicine and of* [3]*Pharmacology, Uniformed Services University of The Health Sciences, Bethesda, Maryland; and* [4]*United States Army Institute of Surgical Research, San Antonio, Texas*

Submitted 25 August 2005; accepted in final form 15 March 2006

Kiang, Juliann G., Phillip D. Bowman, Xinyue Lu, Yansong Li, Xuan Z. Ding, Baiteng Zhao, Yuang-Taung Juang, James L. Atkins, and George C. Tsokos. Geldanamycin prevents hemorrhage-induced ATP loss by overexpressing inducible HSP70 and activating pyruvate dehydrogenase. *Am J Physiol Gastrointest Liver Physiol* 291: G117–G127, 2006. First published March 24, 2006; doi:10.1152/ajpgi.00397.2005.—Hemorrhage in mice results in decreased ATP levels in the jejunum, lung, kidney, heart, and brain but not in liver tissue lysates, albeit at variable levels and time kinetics. The decreased protein expression and activity of pyruvate dehydrogenase (PDH) accounted for the hemorrhage-induced ATP loss. Treatment with geldanamycin (GA; 1 μg/g body wt), a known inducer of heat shock protein (HSP)70, inhibited the hemorrhage-induced ATP loss in the jejunum, lung, heart, kidney, and brain. GA was found to increase PDH protein, preserve PDH enzymatic activity, and inhibit mucosal injury in jejunum tissues. GA-induced HSP70i was found to form complexes with PDH protein. HSP70 gene transfer into intestinal epithelial cells promoted PDH and ATP levels, whereas HSP70 short interfering RNA limited them. We conclude that agents able to increase the expression of HSP70 and PDH may be of value in reducing pathology resulting from hemorrhage-associated ATP loss.

heat shock protein 70; intestine

HEMORRHAGE is often associated with systemic inflammatory response syndrome (SIRS), multiple organ dysfunction (MOD), and multiple organ failure (MOF) (3, 12), and the documented loss of ATP is believed to play a central role in tissue pathology. Interference with the synthesis of ATP in mitochondria results in cell apoptosis, and, therefore, inhibition of ATP loss may prevent hemorrhage-associated clinical manifestations (1, 12). The addition of ATP-$MgCl_2$ (23) and ethyl pyruvate (7) in resuscitation fluids has been shown to maintain tissue ATP levels and limit tissue injury. Geldanamycin (GA), an inducible heat shock protein 70 kDa (HSP70i) and an inducible nitric oxide synthase (iNOS) inhibitor, can block the expression of iNOS and its transcriptional enhancer Kruppel-like factor (KLF)6 in organs of mice subjected to hemorrhage. GA-induced HSP70i formed complexes with iNOS and KLF6 (13, 14).

The mechanisms that underlie the ATP loss observed in organs of animals after significant hemorrhage are not clear. It is known that Ca^{2+} and Na^{+} break the high-energy bond of the ATP molecule, whereas K^{+} and Mg^{2+} help rebuild it (26). It is possible, therefore, that increases in intracellular Ca^{2+} concentration induced by hypoxia under hemorrhagic shock conditions lead to hydrolysis of ATP molecules. The alternative possibility is that the expression of pyruvate dehydrogenase (PDH) and its enzymatic activity are altered by hemorrhage, an aspect that has not been studied before. PDH is the enzyme that converts pyruvate to acetyl CoA, which enters the tricarbonic acid cycle, through which significant amounts of ATP are generated (29). Any reduction of PDH protein and/or its enzymatic activity could result in a reduction of ATP. On the other hand, increased PDH protein or its enzymatic activity could increase ATP levels.

We hypothesized that treatment with GA could block the hemorrhage-induced ATP loss by altering the expression of HSP70i and the expression and activity of PDH that lead to prevention of organ injury. In this study, we found that hemorrhage reduced ATP in various mouse organs and reduced PDH protein and enzymatic activity. GA treatment prevented the hemorrhage-induced ATP loss and organ injury probably by inducing the expression of HSP70i and PDH and by activating PDH.

METHODS

This research was conducted in compliance with the Animal Welfare Act and other Federal statutes and regulations relating to animals and experiments involving animals and adheres to the principles stated in the National Institutes of Health *Guide for the Care and Use of Laboratory Animals*.

Experimental protocol. Experiments were conducted using the mouse model described by Song et al. (28). Male Swiss Webster mice weighing 25–35 g were briefly anesthetized with isoflurane, and 40% of the calculated blood volume was removed over a 1-min period by cardiac puncture with a 26-gauge needle. Mean arterial blood pressure fell from 80 to 40 mmHg in the 2 h after treatment. Treated mice were allowed to respond for 1, 3, 6, 12, 24, and 48 h. Sham-treated animals underwent cardiac puncture, but no blood was removed. In different experiments, mice were pretreated with 10% DMSO-saline or GA (1 μg/g body wt) in 10% DMSO-saline by an intraperitoneal injection 16 h before hemorrhage (25). These mice were then subjected to 40% hemorrhage and allowed to respond for 6 h before they were killed. A small portion of the lung, jejunum, kidney, heart, brain, and liver was removed from the treated mice and frozen immediately at −70°C until it was used for immunoblotting and biochemical assays. Another set of tissues was used for histology examination.

Tissues were minced, sonicated for 15 s, and then centrifuged at 10,000 *g* for 10 min. The supernatant was saved so that the the total amount of protein in each lysate sample could be determined and

Address for reprint requests and other correspondence: J. G. Kiang, Dept. of Cellular Injury, Walter Reed Army Institute of Research, 503 Robert Grant Ave., Rm. 1N07, Silver Spring, MD 20910-7500 (e-mail: Juliann.Kiang@na.amedd.army.mil).

The costs of publication of this article were defrayed in part by the payment of page charges. The article must therefore be hereby marked "*advertisement*" in accordance with 18 U.S.C. Section 1734 solely to indicate this fact.

Report Documentation Page

Form Approved
OMB No. 0704-0188

1. REPORT DATE	2. REPORT TYPE	3. DATES COVERED
01 JUL 2006	**N/A**	**-**

4. TITLE AND SUBTITLE	5a. CONTRACT NUMBER
Geldanamycin prevents hemorrhage-induced ATP loss by overexpressing inducible HSP70 and activating pyruvate dehydrogenase	5b. GRANT NUMBER
	5c. PROGRAM ELEMENT NUMBER
6. AUTHOR(S)	5d. PROJECT NUMBER
Kiang J. G., Bowman P. D., Lu X., Li Y., Ding X. Z., Zhao B., Juang Y. T., Atkins J. L., Tsokos G. C.,	5e. TASK NUMBER
	5f. WORK UNIT NUMBER
7. PERFORMING ORGANIZATION NAME(S) AND ADDRESS(ES)	8. PERFORMING ORGANIZATION REPORT NUMBER
United States Army Institute of Surgical Research, JBSA Fort Sam Houston, TX 78234	
9. SPONSORING/MONITORING AGENCY NAME(S) AND ADDRESS(ES)	10. SPONSOR/MONITOR'S ACRONYM(S)
	11. SPONSOR/MONITOR'S REPORT NUMBER(S)

12. DISTRIBUTION/AVAILABILITY STATEMENT
Approved for public release, distribution unlimited

13. SUPPLEMENTARY NOTES

14. ABSTRACT

15. SUBJECT TERMS

16. SECURITY CLASSIFICATION OF:			17. LIMITATION OF ABSTRACT	18. NUMBER OF PAGES	19a. NAME OF RESPONSIBLE PERSON
a. REPORT	b. ABSTRACT	c. THIS PAGE			
unclassified	**unclassified**	**unclassified**	**SAR**	**11**	

immunoblot analysis performed. The cellular ATP and PDH levels were measured. Proteins and moieties were assessed by immunoprecipitation and immunoblotting between HSP70i and PDH.

Histopathological assessment. Small intestinal tissue specimens were rinsed in cold saline solution and immediately fixed in 10% buffered formalin phosphate. The tissue was then embedded in paraffin, sectioned transversely, and stained with hematoxylin-eosin. The mucosal crypt depth and width and villus height were measured. Mucosal damage for each slide was graded on the six-tiered scale defined by Chiu et al. (3a), as follows: *grade 0*, normal mucosa; *grade 1*, development of subepithelial spaces near the tips of the villi with capillary congestion; *grade 2*, extension of the subepithelial space with moderate epithelial lifting from the lamina propria; *grade 3*, significant epithelial lifting along the length of the villi with a few denuded villus tips; *grade 4*, denuded villi with exposed lamina propria and dilated capillaries; and *grade 5*, disintegration of the lamina propria, hemorrhage, and ulceration.

Cell culture. Human intestinal epithelial T84 cells, FHs74 Int cells, and CRL-1550 cells (American Type Cell Culture; Rockville, MD) were grown in DMEM, hybrid-care medium, and RPMI 1640, respectively, in a humidified incubator with a 5% CO_2 atmosphere. Each medium was supplemented with 2 mM glutamine, 4.5 g/l glucose, 10% FBS, 100 U/ml penicillin, and 100 μg/ml streptomycin; pH 7.4 (Quality Biological; Gaithersburg, MD). Cells were fed every 3–4 days.

HSP70 short interfering RNA transfection. To decrease HSP70 protein, RNA interference technology was used. Two designed pairs of oligoduplexes targeted against HSP70 (GenBank Accession No. NM_005346) were purchased from Qiagen (Valencia, CA). The target sequences of those oligoduplexes are 5′-AAG GGU GUU UCG UUC CCU UUA-3′ and 5′-AAC CGA UAU GUU CAU UAG AAU-3′, respectively. A nonspecific oligoduplex (nonsilencing control, targeting on 5′-AAU UCU CCG AAC GUG UCA CGU-3′) at the same final concentrations as the HSP70 RNA duplexes was used as a negative control. To maximize the short interfering (si)RNA silencing potential, siRNAs were heated for 1 min at 90°C followed by 60 min at 37°C before the siRNA transfection. Interested cells were grown in fresh medium without antibiotics for 24 h before the transfection. These cells were then transferred to each well in six-well plates (density: 2×10^6 cells/well). The transient transfections with 50, 100, and 200 nM of each siRNA duplex were performed using Lipofectamine reagent (Invitrogen; Carlsbad, CA) according to the manufacturer's protocol. Cells were harvested and assayed 24 h after transfection.

HSP70 and iNOS gene contstructs. Two genes encoding HSP70 and iNOS were used in this study. The *HSP70* gene (a gift from Dr. Richard I. Morimoto) was first cloned in 1985 (10). The full length of the *HSP70* gene contains 2,400 bp, and this gene was inserted with the enzymes *Bam*H1 and *Eco*RI in the pH 2.3 plasmid. cDNA of human iNOS was obtained from Dr. N. Tony Eissa (Baylor College of

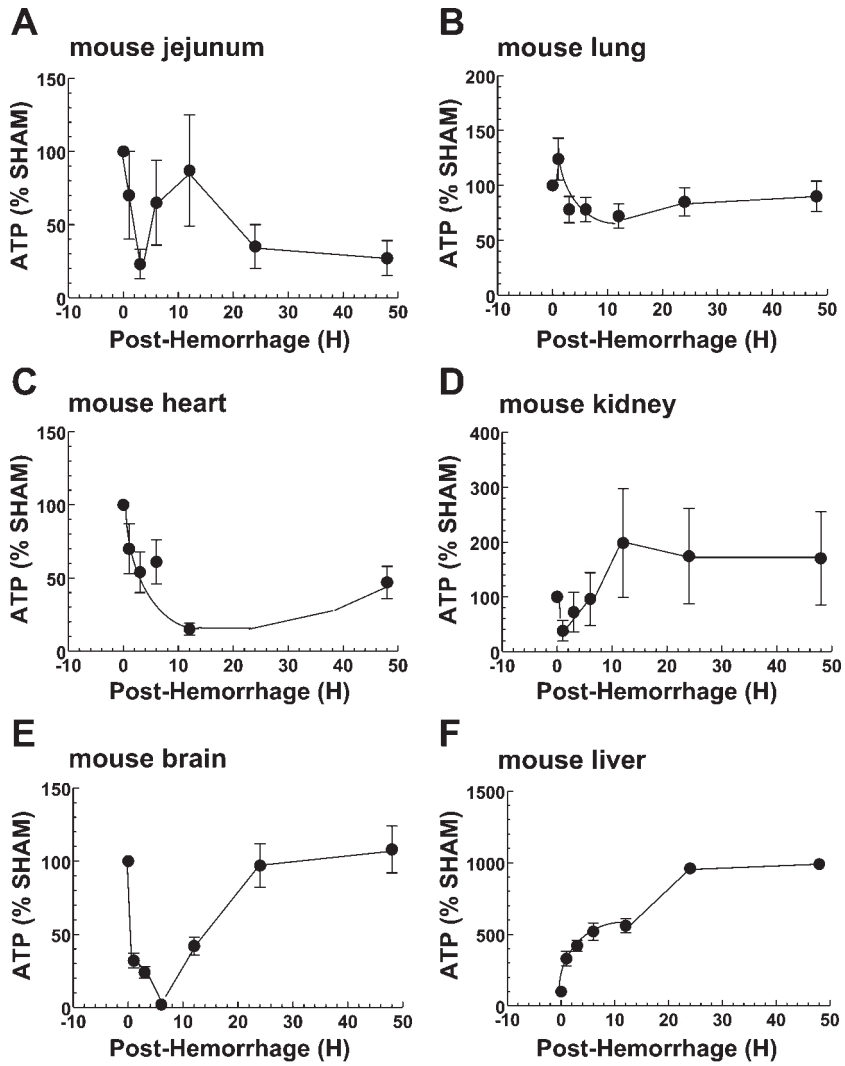

Fig. 1. Time course of ATP levels in lysates of organs of mice subjected to hemorrhage. Mice were exposed to hemorrhage and allowed to respond for 1, 3, 6, 12, 24, or 48 h ($n = 6$). ATP levels in lysates of the jejunum (*A*), lung (*B*), heart (*C*), kidney (*D*), brain (*E*), and liver (*F*) were measured. Data collected from hemorrhaged organs were normalized to those from sham-operated organs (%Sham).

Medicine, Houton, TX) and was first published in 2001 (8). A 3,362-bp coding sequence with *Hin*dIII and *Xho*I restriction sites at each terminal of the human *iNOS* gene was subcloned from this full length of human iNOS cDNA. Using PCR application, the forward and reverse primers were 5′-CT AAG CTT GTC ATG GCC TGT CCT TGG AAA TTT CTG TTC-3′ and 5′-GAC TCG AGC TCA GAG CGC TGA CAT CTC CAG GCT-3′, respectively. After digestion and purification of the PCR amplification product, the expression cDNA sequence was used for insertion into the vector. The vector used in this study was pcDNA3 (Invitrogen). The *HSP70* gene was cut with the enzymes *Bam*HI and *Eco*RI and inserted into the pcDNA3 vector with T4 DNA ligase (5). The expression cDNA of the *iNOS* gene was inserted between the *Hin*dIII and *Xho*I sites of the pcDNA 3.1 vector. The expression construct was then sequenced to confirm its correct sequence and open reading frame.

Transient gene transfection. Cultured cells (1.5×10^6) were grown in six-well plates. Cells in each well were treated with 4 μg iNOS or HSP70 expression plasmid in 0.5 ml of antibiotics-free growth medium using the Lipofectamine 2000 Transfection Kit (Invitrogene). An equal amount of cells was also mixed with blank pcDNA 3.1 vector as the control group. Then, 1.5 ml of DMEM were added to each well, and cells were placed back to the incubator for 24 h to allow the transient transfection.

Immunoprecipitation. Tissue lysates containing 300 μg protein were incubated with the specified antibody (5 μl), chilled on ice for 1 h, mixed with protein A/G agarose beads (50 μl, Santa Cruz Biotechnology; Santa Cruz, CA), and incubated overnight on a nutator at 4°C. The immunoprecipitate was collected by centrifugation at 12,500 *g* for 10 min and washed twice with 500 μl of stop buffer and once with 500 μl PBS wash buffer. The pellet was resuspended in 50 μl of electrophoresis sample buffer without 2-mercaptoethanol, boiled for 5 min, and then centrifuged for 30 s to remove the agarose beads. The supernatant was incubated with 5% 2-mercaptoethanol at 37°C for 1 h. Twenty-five microliters of sample were loaded onto precast 10% Tris-glycine polyacrylamide gels for Western blots.

Western blot analysis. Samples were resolved on SDS-polyacrylamide slab gels (precast 10% gel, Invitrogen). Protein was blotted onto a nitrocellulose membrane (type NC, 0.45 μm, Schleicher and Schuell) using a Novex blotting apparatus and the manufacturer's protocol. The nitrocellulose membrane was blocked by incubation for 90 min at room temperature in PBS containing 5% nonfat dried milk. The blot was then incubated for 60 min at room temperature with the selected antibody against actin (Santa Cruz Biotechnology); HSP90, HSP60, and HSP40 (Santa Cruz Biotechnology); HSP70i (Amersham); or PDH (BD Transduction Laboratories; San Diego, CA) at 1 μg/ml in PBS-5% BSA. The blot was washed three times (10 min each) in Tris-buffered saline-0.1% Tween 20 before it was incubated for 60 min at room temperature with a 1,000× dilution of species-specific IgG peroxidase conjugate (Santa Cruz Biotechnology) in PBS-1% gelatin. The blot was washed six times (5 min each) in Tris-buffered saline-0.1% Tween 20 before detection of the peroxi-

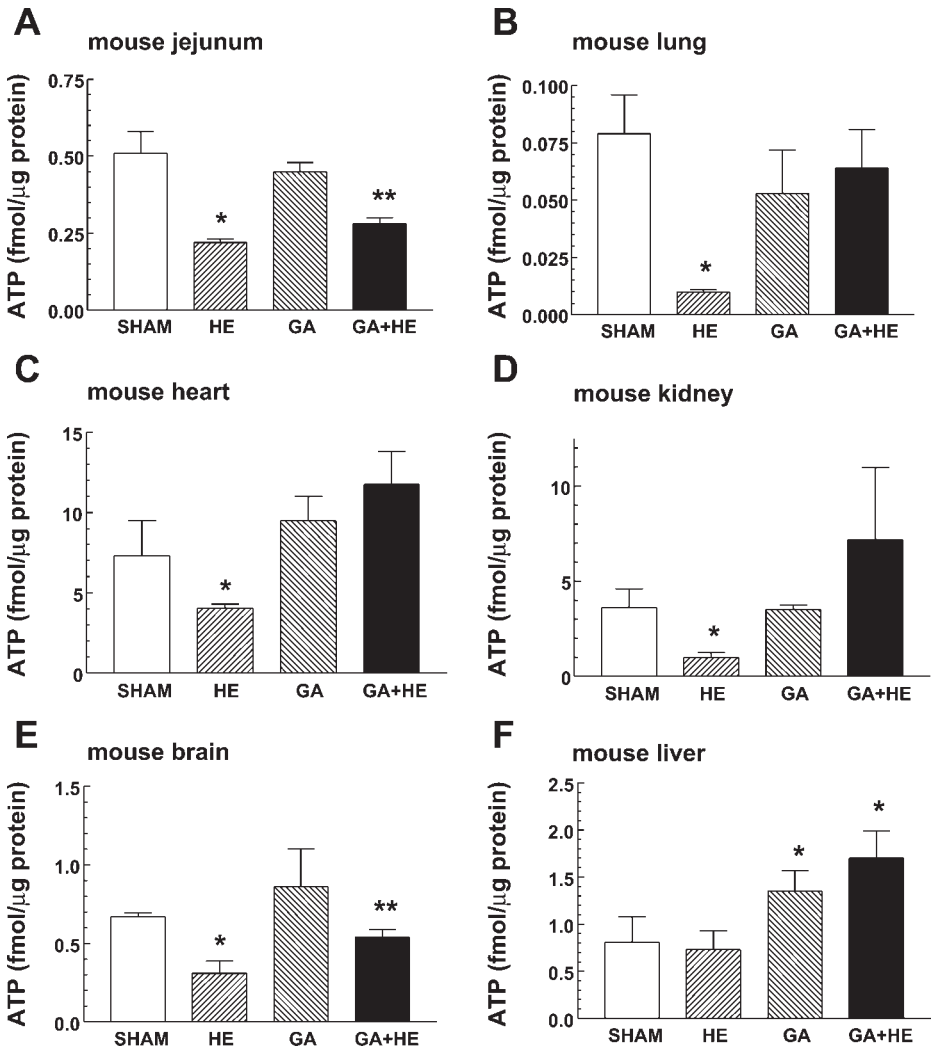

Fig. 2. Geldanamycin (GA) inhibits the hemorrhage (HE)-induced decrease in ATP levels in mouse organs. Mice were treated with GA (1 μg/g body wt) in 10% DMSO-saline by an intraperitoneal injection 16 h before hemorrhage ($n = 3$–5). ATP levels in lysates of the jejunum (*A*), lung (*B*), heart (*C*), kidney (*D*), brain (*E*), and liver (*F*) were measured. *$P < 0.05$ vs. sham, GA, and GA + HE; **$P < 0.05$ vs. sham, HE, and GA (determined by χ^2-test).

dase activity using the Enhanced Chemiluminenscence Kit (Amersham Life Science Products).

Immunofluorescent staining for confocal microscopy. Cells (1×10^5) were plated on a glass coverslip precoated with poly-L-lysine. After attachment, cells were fixed with 3.7% formaldehyde and permeabilized with 0.1% Triton X-100 in PBS for 10 min. Permeabilized cells were blocked with 2% BSA for 30 min and incubated with a mouse anti-human PDH monoclonal antibody (1:200 dilution, Molecular Probes) or a rabbit anti-human HSP70 polyclonal antibody (Upstate) at a dilution of 1:200 in PBS containing 2% BSA for 1 h. Cells were then incubated for 1 h with Alexa Fluor 488 goat anti-mouse IgG (1:400, Molecular Probes) and Alexa Fluor 594 goat anti-rabbit IgG (1:400 dilution, Molecular Probes). Between each step, three washes with PBS were applied. After being stained with antibodies, cells were mounted using a SlowFade Light Antifade Kit with 4′,6-diamidino-2-phenylindole (Molecular Probes) on a glass slide and inspected microscopically under a laser confocal scanning.

Measurements of cellular ATP level. Cellular ATP levels were determined using the ATP Bioluminescence Assay Kit HS II (Roche; Mannheim, Germany). Luminescence was measured with a TD-20/20 luminometer (Turner Designs; Sunnyvale, CA). Data were normalized to total protein, and the cellular ATP level is expressed as femtomoles per microgram of protein.

Measurements of PDH activity. The cell lysate in the assay buffer containing 1 mM DTT and PMSF was incubated with 0.2 mM Na^+-CoA for 15 min at 37°C. The mixture was then mixed with 1.25 mM oxaloacetate and 1.25 μg 5,5-dithiobia(2-nitrobenzoic acid) and incubated for 10 min at 37°C. The final mixture was mixed with 5 units citrate synthase and read immediately at 412 nm at 30°C. The activity was normalized with the total protein concentration, and the specific activity is presented as microunits per microgram of protein.

Measurement of cell viability. Cell viability was determined by the trypan blue exclusion assay. Twenty microliters of cell suspension were mixed with 20 μl of 0.4% trypan blue solution (Sigma Chemical; St. Louis, MO). The viability was calculated accordingly (16).

Solutions. Na^+-Hanks' solution contained (in mM) 145 NaCl, 4.5 KCl, 1.3 $MgCl_2$, 1.6 $CaCl_2$, and 10 HEPES (pH 7.40 at 24°C). High-K^+-Hanks' solution contained (in mM) 124.5 NaCl, 25 KCl, 1.3 $MgCl_2$, 1.6 $CaCl_2$, and 10 HEPES (pH 7.40 at 24°C). Mg^{2+}-free Hanks' solution contained (in mM) 146.3 NaCl, 4.5 KCl, 1.6 $CaCl_2$, and 10 HEPES (pH 7.40 at 24°C). Ca^{2+}-free Hanks' solution was prepared by adding 10 mM EGTA to nominally Ca^{2+}-free Hanks' solution. To remove external Na^+, an equal molar of *N*-methyl-D-glucamine was used to replace Na^+. The PDH assay buffer contained (in mM) 50 Tris·HCl, 10 Na^+ pyruvate, 2 NAD^+, 2 thiamine pyrophosphate, 1 $MgCl_2$, 1 DTT, and 1 PMSF (pH 7.40 at 24°C). Stop buffer contained 50 mM Tris·HCl, 1% Nonidet P-40, 0.25% Na^+ deoxycholate, 150 mM NaCl, 1 mM EDTA, 1 mM PMSF, 1 mM Na_3VO_4, 1 mM NaF, and 1 μg/ml of aprotinin, leupeptin, and pepstatin.

Statistical analysis. All data are expressed as means ± SE. One-way ANOVA, two-way ANOVA, Studentized-range test, Bonferroni's inequality, and χ^2-test were used for comparison of groups with 5% as the significance level.

Chemicals. GA was obtained from Sigma.

RESULTS

Hemorrhage decreases ATP levels in mouse organs. Hemorrhage results in decreased ATP levels in lung, ileum, and liver tissues (2, 3, 3a, 11–14, 24), but the time course of the decrease has not been studied. Figure 1 demonstrates how hemorrhage affects the ATP level in a mouse hemorrhage model over time. In the mouse jejunum, ATP levels decreased within the first hour, returned to baseline at 12 h, but decreased again thereafter (Fig. 1*A*). In lung (Fig. 1*B*) and heart (Fig. 1*C*) tissues, ATP levels decreased steadily within the first 12 h and remained low afterward. In contrast, ATP levels in the brain (Fig. 1*E*) decreased and reached the lowest point within 8 h and then returned to the baseline level at 24 h. In the kidney (Fig. 1*D*), ATP levels decreased within 1 h, returned to baseline by the sixth hour, and remained at the baseline to 48 h. Unlike the jejunum, lung, heart, brain, and kidney, ATP levels in the liver (Fig. 1*F*) increased after hemorrhage and reached maximal levels at 24 h.

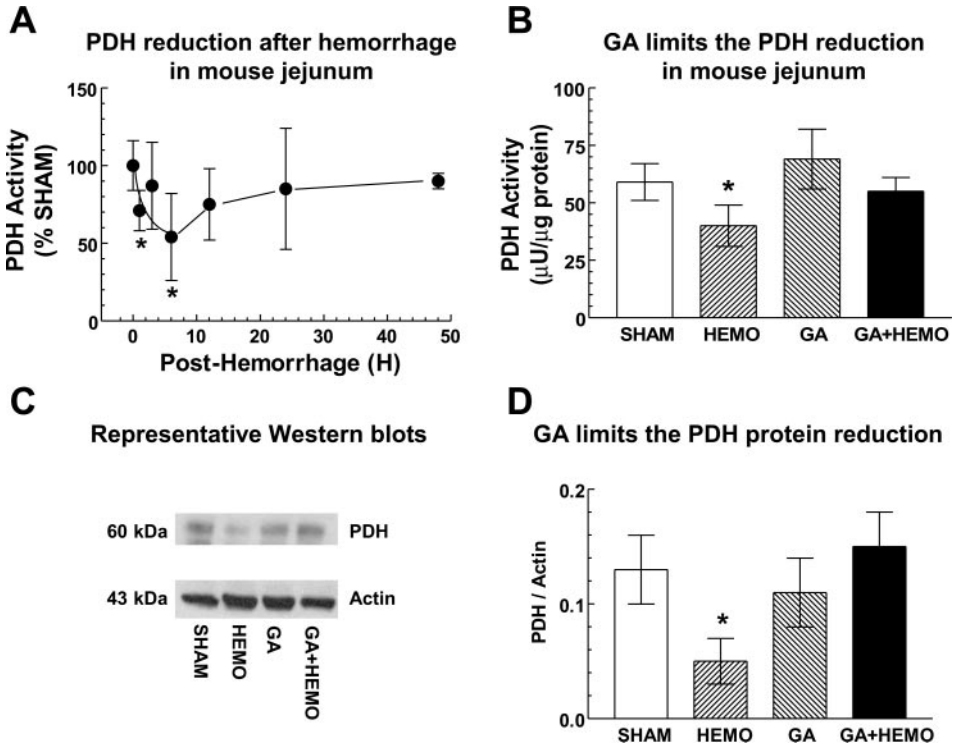

Fig. 3. GA limits the hemorrhage (HEMO)-induced pyruvate dehydrogenase (PDH) activity decrease. *A*: mice were subjected to hemorrhage and allowed to respond for 1, 3, 6, 12, 24, or 48 h ($n = 6$). PDH activities in lysates of the hemorrhaged jejunum (HEMO) were measured. Data collected from the hemorrhaged jejunum were normalized to those from the sham-operated jejunum. *$P < 0.05$ vs. *time 0* (determined by one-way ANOVA and Bonferroni's inequality). *B*: mice were pretreated with GA (1 μg/g body wt) in 10% DMSO-saline by an intraperitoneal injection 16 h before hemorrhage ($n = 3$–5). PDH activities in lysates of the hemorrhaged jejunum were measured. *$P < 0.05$ vs. sham, GA, and GA + HEMO (determined by χ^2-test). *C*: representative Western blots of PDH. *D*: the protein bands of PDH were quantitated densitometrically and normalized to that of actin. *$P < 0.05$ vs. sham, GA, and GA + HEMO (determined by χ^2-test).

Treatment with GA inhibits hemorrhage-induced ATP loss in mouse organs. We treated mice with GA 16 h before subjecting them to hemorrhage to determine whether it affected ATP levels in various tissues. Figure 2 shows that treatment with GA significantly limited ATP loss in jejunum (Fig. 2*A*) and brain (Fig. 2*E*) tissues and fully blocked ATP loss in lung (Fig. 2*B*), heart (Fig. 2*C*), and kidney (Fig. 2*D*) tissues. GA treatment further increased ATP levels in the liver (Fig. 2*F*).

Hemorrhage reduces PDH activity in the jejunum. Because it has been reported that increases in ATP levels mediated by PDH improved heart function and metabolism after hemorrhagic shock (18), we sought to determine whether the PDH activity changed in the organs of mice subjected to hemorrhage. Figure 3*A* demonstrates that hemorrhage causes a significant decrease in PDH activity in the jejunum at 6 h. PDH activity returned to the baseline level at 24 h.

GA inhibits the hemorrhage-induced decrease in PDH activity and protein expression in the jejunum. Because GA treatment was shown above to prevent the hemorrhage-induced ATP loss, we considered it likely that GA also prevented the

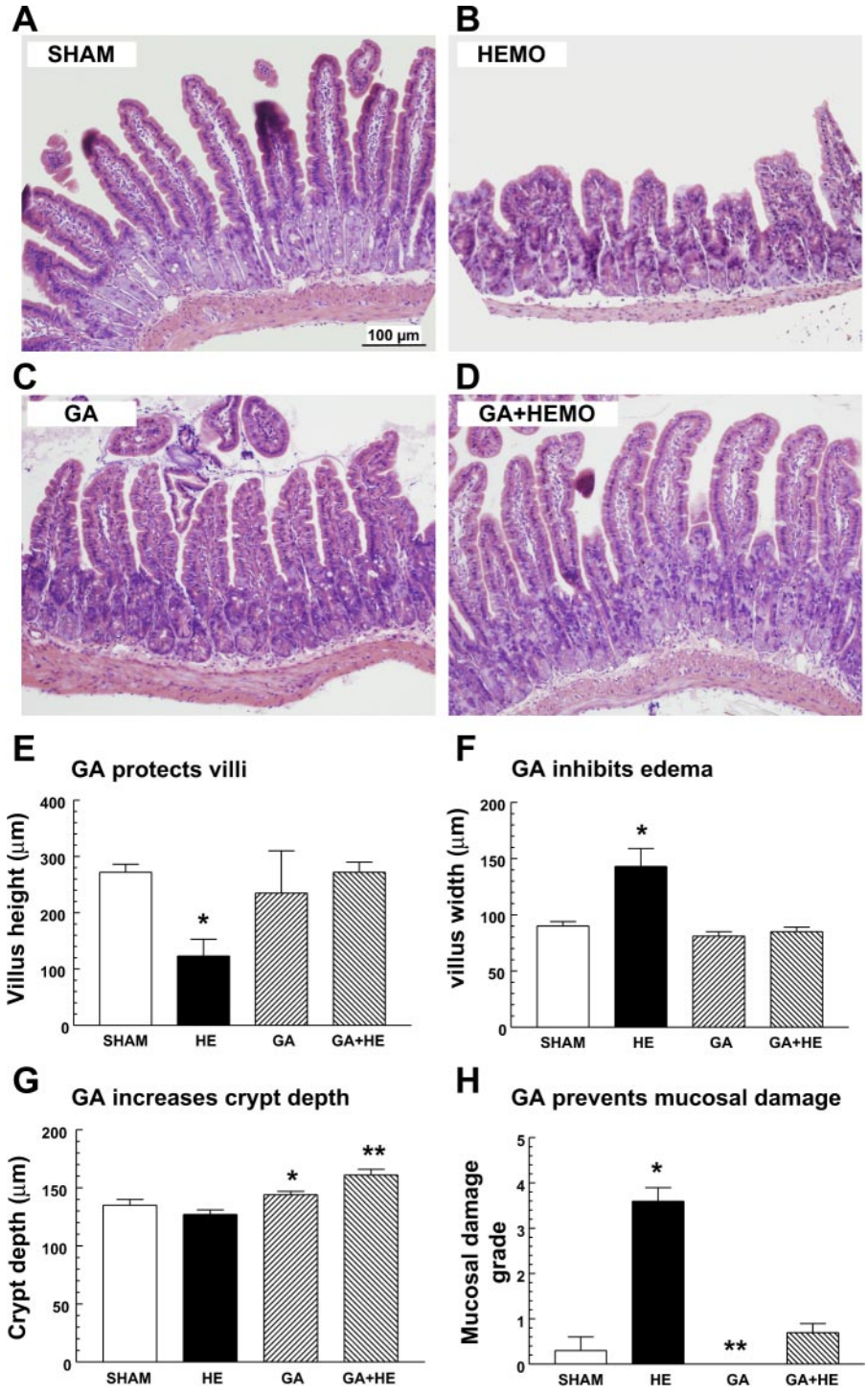

Fig. 4. GA prevents hemorrhage-induced intestinal tissue damage. *A–D*: low-power photomicrographs of full-thickness sections of the jejunum of a sham-treated mouse (*A*), a mouse subjected to hemorrhage (*B*), a GA-treated mouse (*C*), and a mouse treated with GA before hemorrhage (*D*). *E–G*: villus height (*E*) and width (*F*) and crypt depth (*G*) were measured. *H*: the histological severity of injury grade for each tissue section was as follows: sham, 0.3 ± 0.3; HEMO, 3.6 ± 0.3; GA, 0; and GA + HEMO, 0.7 ± 0.2. *$P < 0.05$ vs. sham, HEMO, and GA + HEMO; **$P < 0.05$ vs. sham, HEMO, and GA (determined by χ^2-test).

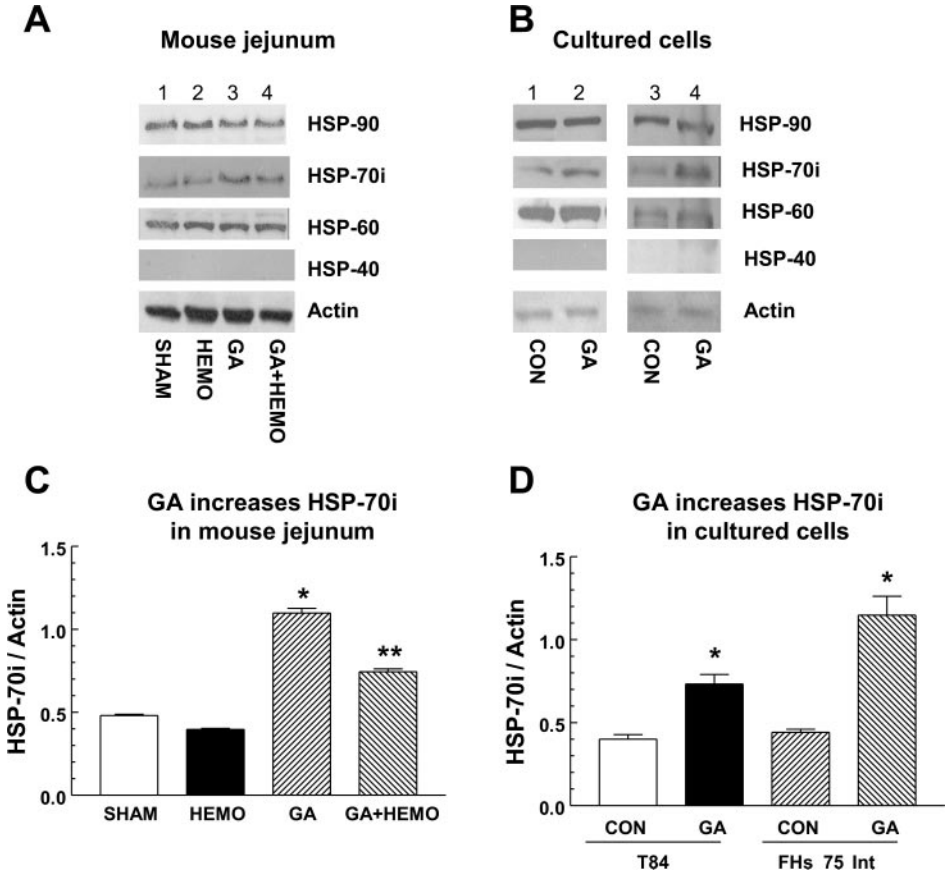

Fig. 5. GA increases inducible heat shock protein 70 kDa (HSP)70 inducer (HSP70i) in the mouse jejunum and in cultured cells. *A* and *C*: mice were pretreated with GA (1 μg/g body wt) in 10% DMSO-saline by an intraperitoneal injection 16 h before hemorrhage ($n = 3$–5). *A*: representative Western blots of jejunum HSP90, HSP70i, HSP60, HSP40, and actin; *C*: HSP70i and actin were quantitated densitometrically. $*P < 0.05$ vs. sham, HEMO, and GA + HEMO; $**P < 0.05$ vs. sham, HEMO, and GA (determined by χ^2-test). *B* and *D*: both T84 and FHs75 Int cells were treated with GA (1 μM, 16 h, $n = 3$). *B*: representative Western blots of cellular HSP90, HSP70i, HSP60, HSP40, and actin; *D*: HSP70i and actin were quantitated densitometrically. CON, control. $*P < 0.05$ vs. sham (determined by Student's *t*-test).

hemorrhage-induced decrease in the PDH activity. Although GA treatment alone did not alter PDH activity, it prevented the hemorrhage-induced decrease in PDH activity in jejunum tissue lysates (Fig. 3*B*). Immunoblot experiments showed that hemorrhage decreased the PDH protein level, and GA treatment prevented the decrease (Fig. 3, *C* and *D*), suggesting that the decreased PDH activity is as a result of the decreased PDH protein level and that GA prevents the decrease.

GA increases survival from hemorrhagic shock and prevents hemorrhage-induced organ injury. Six hours after hemorrhage, mice displayed 60% survival. In the presence of GA, 84% of hemorrhaged mice survived. Histological assessment of mouse

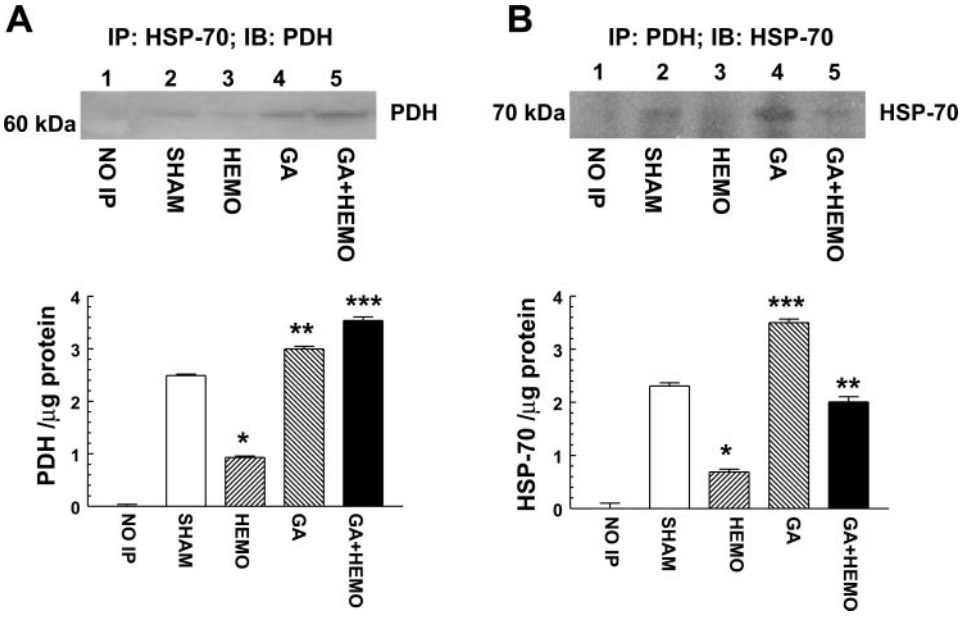

Fig. 6. GA-induced increases in HSP70i lead to formation of PDH-HSP70 complexes. Mice were pretreated with GA (1 μg/g body wt) in 10% DMSO-saline by an intraperitoneal injection 16 h before hemorrhage ($n = 3$–5). *A*: representative Western blot (*top*) of jejunum HSP70i complex formation with PDH. Lysates of mouse jejunum were immunoprecipitated (IP) with anti-HSP70i antibody, and PDH was then detected with anti-PDH antibody using immunoblot (IB) analysis. *B*: representative Western blot (*top*) of jejunum PDH complex formation with HSP70i. Lysates of mouse jejunum were immunoprecipitated with anti-PDH antibody, and HSP70i was then detected with anti-HSP70i antibody using immunoblot analysis. $*P < 0.05$ vs. sham, GA, and GA + HEMO; $**P < 0.05$ vs. sham, HEMO, and GA; $***P < 0.05$ vs. sham, HEMO, GA + HEMO (determined by χ^2-test). No IP, normal mouse serum with no antibody added for immunoprecipitation.

jejunum tissue showed that hemorrhage reduced the villus height (Fig. 4, *B* and *E*) and increased the villus width (Fig. 4, *B* and *F*) without altering the crypt depth (Fig. 4, *B* and *G*), suggesting the presence of edema. The mucosal damage grade on the hemorrhaged jejunum was 3.6 ± 0.3 ($P < 0.05$ vs. sham; Fig. 4*H*).

GA treatment alone did not alter the villus height (Fig. 4, *C* and *E*), villus width (Fig. 4, *C* and *F*), or crypt depth (Fig. 4, *C* and *G*). However, GA treatment before hemorrhage protected the jejunum (Fig. 4, *D–G*), and the mucosal damage grade was reduced to the level recorded in control animals (Fig. 4*H*).

GA upregulates HSP70i in the jejunum and in cultured cells. Using immunoblot analysis, HSP90, HsP70i, and HSP60, but not HSP40, were detected in the sham-treated mouse jejunum. Hemorrhage did not alter these HSPs. GA treatment increased HSP70i expression but not that of HSP90 and HSP60 (Fig. 5, *A* and *C*). Similar findings were obtained with T84 cells and FHs75 Int cells (Fig. 5, *B* and *D*).

HSP70 forms complexes with PDH in the jejunum. When jejunum tissue lysates were immunoprecipitated with anti-HSP70 antibody and the precipitates were immunoblotted with anti-PDH antibody, the PDH band was detected (Fig. 6*A*), but bands of HSP90, HSP60, and HSP40 were not found (data not shown). When lysates were immunoprecipitated with anti-PDH antibody and the precipitates were then blotted with anti-HSP70 antibody, the HSP70 band was detected (Fig. 6*B*). The intensity of each band indicated that GA treatment increased PDH and HSP70 proteins (Fig. 6). No HSP90, HSP60, or HSP40 bands were detected (data not shown). Therefore, our data indicate that HSP70 can form a complex with PDH.

HSP70 overexpression increases ATP and PDH in cultured cells. GA is a HSP70i inducer and an iNOS inhibitor (12–14). To distinguish which of the two functions of GA contributed to its inhibitory actions on cellular ATP and PDH reduction caused by hemorrhage, we studied cultured intestinal epithelial T84 cells transiently transfected with either iNOS or HSP70 expression vectors (Fig. 7, *A* and *B*) to determine the effect of forced expression of these genes on ATP levels (Fig. 7*D*), PDH expression (Fig. 7*C*), and PDH enzymatic activity (Fig. 7*E*). The *HSP70* gene-transfected cells displayed a significantly higher ATP basal level than the control, vector-transfected, and *iNOS* gene-transfected cells (Fig. 7*D*). Similarly, PDH protein and its enzymatic activity in HSP70 gene-transfected cells were significantly greater than in vector-transfected cells (Fig. 7, *C* and *E*). Similar effects were found with cultured small intestinal cells (Fig. 8*A*).

To further confirm that the level of HSP70 present in cells can influence the levels of PDH and ATP, HSP70 RNA interference technology was used. Cells were treated with 50, 100, or 200 nM siRNA for 24 h. siRNA at 50 and 100 nM failed to inhibit ATP (data not shown), whereas at 200 nM, it significantly decreased HSP70 protein, PDH protein and activity, and the cellular ATP level (Fig. 8*B*). These experiments strongly suggest that overexpression of HSP70 rather than iNOS accounts for increases in ATP levels.

HSP70 and PDH form complexes in cultured cells. We next wanted to confirm the observed association between HSP70

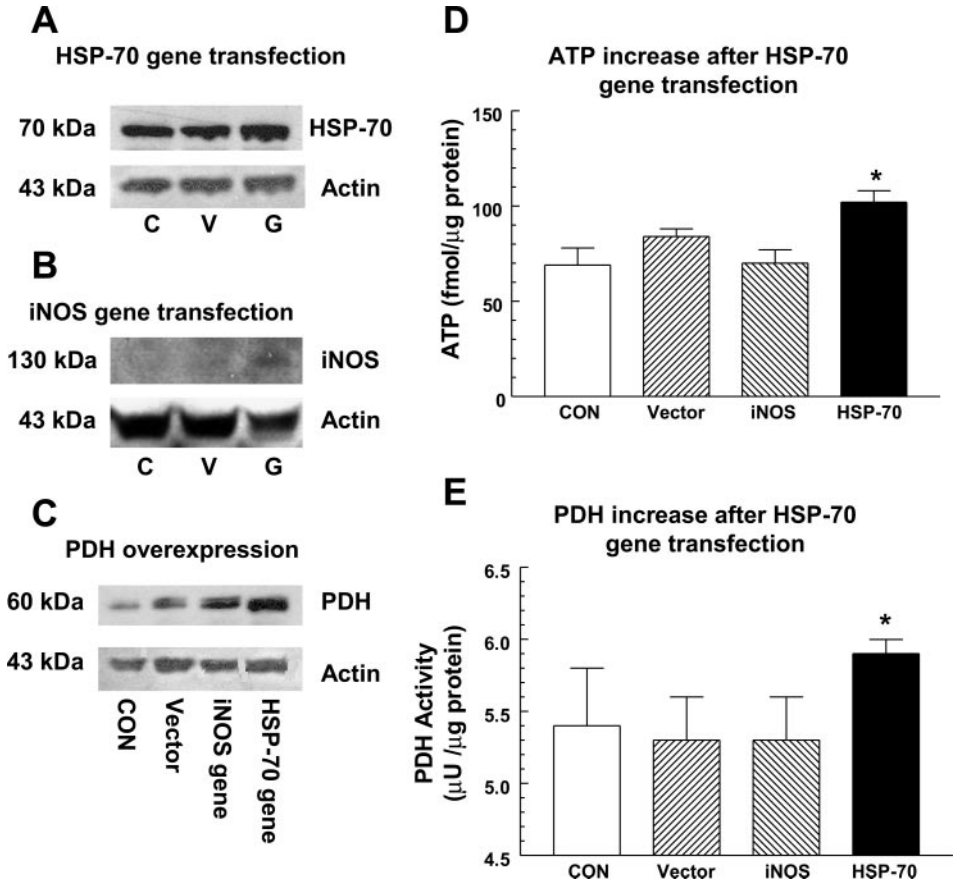

Fig. 7. Overexpression of HSP70 increases ATP levels and PDH activity. T84 cells were transfected with vector (V) alone or with HSP70 or inducible nitric oxide synthase (iNOS) expression vectors (G) for 16 h before ATP and PDH were measured ($n = 3$) or were left untransfected [control (C)]. *A*: representative Western blot of HSP70 overexpression after *HSP70* gene transfection. *B*: representative Western blot of iNOS overexpression after *iNOS* gene transfection. *C*: representative Western blot of PDH overexpression after *HSP70* gene transfection. *D*: increases in ATP after *HSP70* gene transfection. *E*: increases in PDH activity after *HSP70* gene transfection. *$P < 0.05$ vs. control, vector, and *iNOS* gene transfer (determined by χ^2-test).

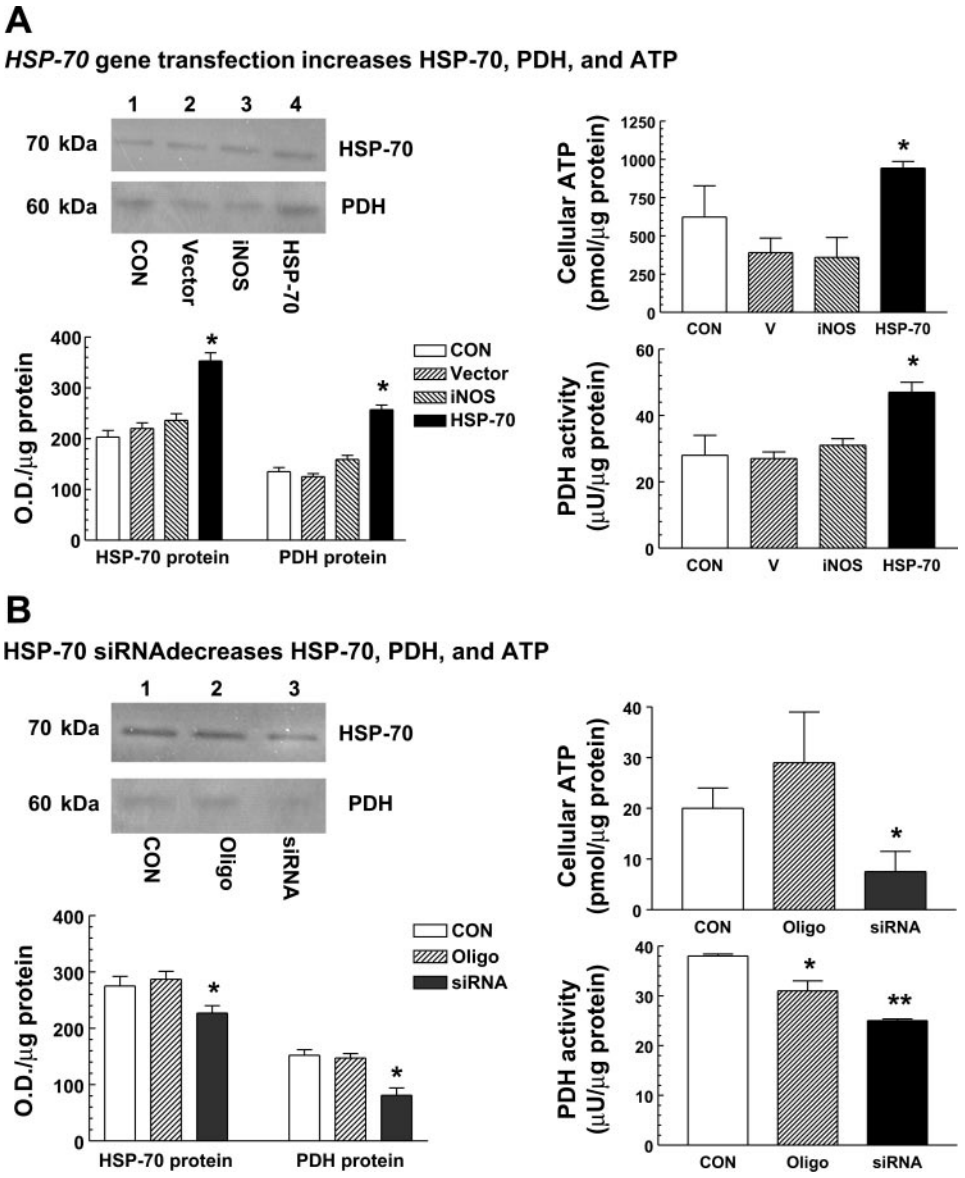

Fig. 8. HSP70 changes ATP levels and PDH activity. FHs75 Int cells were transfected with empty vector alone or with *iNOS* or *HSP70* gene expression vectors for 16 h before ATP and PDH were measured ($n = 3$) or were left untransfected. *A*: representative Western blots of overexpression of HSP70 and PDH after *HSP70* gene transfection. The overexpression of HSP70 and PDH was quantitated densitometrically [optical densiometry units (OD)]. Increases in cellular ATP and PDH activity after *HSP70* gene transfection are shown. $*P < 0.05$ vs. control, vector, and *iNOS* gene transfer (determined by χ^2-test). *B*: in a parallel experiment, FHs75 Int cells were treated with HSP70 short interfering (si)RNA at 200 nM for 24 h. Oligo, nonsilencing siRNA as a negative control. Representative Western blots of HSP70 and PDH are shown. The protein inhibition of HSP70 and PDH were quantitated densitometrically. Decreases in cellular ATP and PDH activity in cells treated with HSP70 siRNA are shown. $*P < 0.05$ vs. control and oligo (determined by Student's *t*-test).

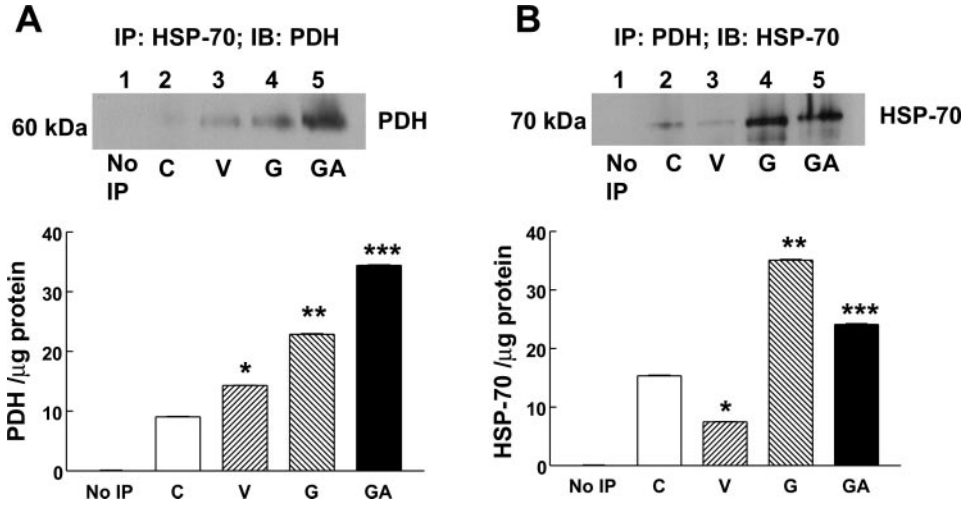

Fig. 9. Both *HSP70* gene transfection and GA-induced increases in HSP70i lead to formation of PDH-HSP70 complexes in T84 cells. T84 cells were transfected with HSP70 vector or vector alone or treated with 1 μM GA for 16 h ($n = 3$). Lysates were prepared for immunoprecipitation and immunoblot analysis. *A*: representative Western blot (*top*) of HSP70i complex formation with PDH. Lysates of T84 cells were immunoprecipitated with anti-HSP70i antibody, and PDH was then detected with anti-PDH antibody using immunoblot analysis. *B*: representative Western blot (*top*) of PDH complex formation with HSP70i. Lysates of T84 cells were immunoprecipitated with anti-PDH antibody, and HSP70i was then detected with anti-HSP70i antibody using immunoblot analysis. $*P < 0.05$ vs. control, gene transfection, and GA; $**P < 0.05$ vs. control, vector, and GA; $***P < 0.05$ vs. control, vector, and gene transfection (determined by one-way ANOVA).

and PDH in jejunum tissues of GA-treated animals. To this end, we induced the expression of HSP70 in T84 intestinal epithelial cells either by transfecting a HSP70 expression vector or by treating them with GA. When T84 cell lysates were immunoprecipiated with anti-HSP70 antibody and the precipitates were blotted with anti-PDH antibody, the PDH band was detected (Fig. 9*A*). When the lysates were immunoprecipitated with anti-PDH antibody and the precipitates were then blotted with anti-HSP70 antibody, the HSP70 band was detected (Fig. 9*B*). The amounts of PDH (Fig. 9*A*, *lane 4* vs. *lane 3*) and HSP70 (Fig. 9*B*, *lane 4* vs. *lane 3*) presented in the complexes also displayed that HSP70 overexpression resulted in increased PDH protein (Fig. 7). These experiments further confirm that HSP70 associates with PDH.

GA increases ATP and PDH in cultured cells. Because the median inhibitory concentration of GA to block hypoxia-induced ATP loss in T84 cells is 0.76 ± 0.24 μM with the correlation coefficient being 0.9163 (J. G. Kiang, unpublished data), cells were treated with GA at 1 μM for 16 h before the detection of HSP70 and PDH. GA treatment induced increases in PDH (Fig. 9*A*, *lane 5* vs. *lane 2*) and HSP70 (Fig. 9*B*, *lane 5* vs. *lane 2*), suggesting that GA increases PDH in addition to HSP70i.

The GA-induced increases in PDH protein (Fig. 10, *A* vs. *B*) and HSP70i protein (Fig. 10, *C* vs. *D*) were further demonstrated with immunofluorescent staining using confocal microscopy. The data clearly showed a colocalization of PDH and HSP70i (Fig. 10, *G* and *H*), further supporting the complex formation between PDH and HSP70i.

GA-induced ATP activity in T84 cells is Na^+ and K^+ dependent. Because the active form of ATP in energy exchange is usually a complex of ATP with Mg^{2+} or Mn^{2+} (29) and because GA decreases intracellular Ca^{2+} concentration (J. G. Kiang, unpublished data), we considered it possible that the GA effect on ATP levels was dependent on ionic compositions in the incubating buffer. Figure 11 shows the effects of various ionic compositions on the ATP level in the absence or presence of GA. When T84 cells were incubated in Na^+-Hanks' solution or ionic-modified buffers, we found that the removal of external Na^+ decreased the ATP basal level, whereas in the presence of 25 mM K^+ (normal is 4.5 mM), the ATP level increased remarkably. Removal of either external Ca^{2+} or external Mg^{2+} did not alter the ATP level. Treatment of cells with GA at 1 μM significantly increased ATP levels in cells bathed in Na^+-containing, Ca^{2+}-free, or Mg^{2+}-free Hanks' solution. GA failed to increase ATP levels in Na^+-free buffer and did not further increase ATP levels in 25 mM

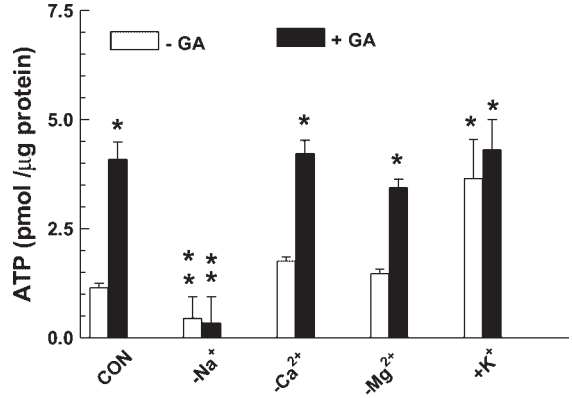

Fig. 11. The GA-induced increase in ATP is Na^+ and K^+ dependent. T84 cells were treated without (−) or with (+) GA (1 μM, 16 h). These cells were then incubated in control buffer or Na^+-free ($-Na^+$), Ca^{2+}-free ($-Ca^{2+}$), Mg^{2+}-free ($-Mg^{2+}$), or 25 mM K^+-containing ($+K^+$) buffer for 1 h. ATP levels in cell lysates were measured ($n = 3$). *$P < 0.05$ vs. control buffer alone, $-Na^+$, $-Na^+$ + GA, $-Ca^{2+}$, and $-Mg^{2+}$; **$P < 0.05$ vs. control buffer alone, +GA alone, $-Ca^{2+}$ + GA, $-Mg^{2+}$ alone, $-Mg^{2+}$ + GA, $+K^+$, and $+K^+$ + GA (determined by two-way ANOVA and Bonferroni's inequality).

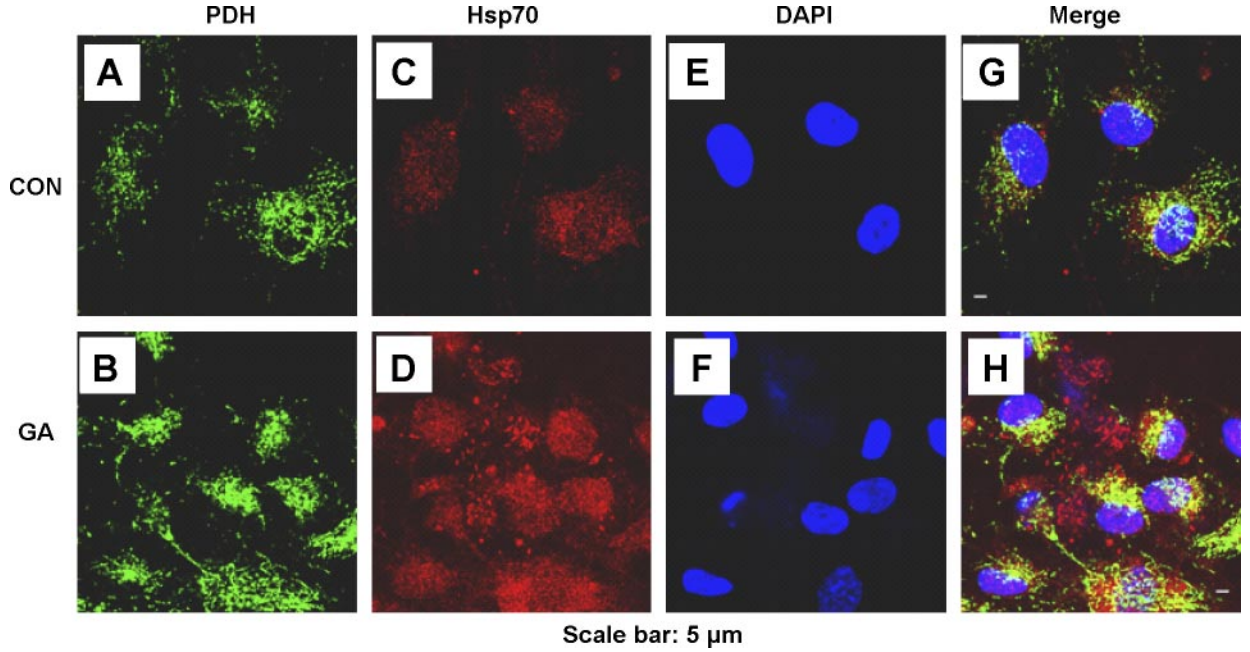

Fig. 10. Colocalization of PDH and HSP70i. FHs75 Int cells were treated with 1 μM GA for 16 h. These cells were stained immunofluorescently with antibodies direct to PDH (*A* and *B*, in green), HSP70 (*C* and *D*, in red), or DAPI (*E* and *F*, in blue). Colocalization of PDH and HSP70i is shown in yellow (*G* and *H*).

K^+-containing buffer, suggesting that the action of GA is mediated by pathways involving Na^+ and K^+.

DISCUSSION

MOF is known to occur after hemorrhagic shock (1, 12), and a role has been assigned to the increased caspase-3 activity and reduction of ATP levels after hemorrhage (13–15). Proteolytic fragments derived as a result of caspase-3-mediated cleavage are cleared up by the proteasome complex (6).

In the present study, hemorrhage decreased ATP levels in jejunum, lung, heart, kidney, and brain tissue lysates. ATP levels in brain and kidney tissues returned to basal levels, whereas in the jejunum, lung, and heart, ATP levels remained below the basal levels. Although the hemorrhage-associated low levels of ATP in the jejunum, lung, and heart have been proposed to be responsible for the delayed hemorrhage manifestations such as MOD and MOF, the exact mechanism(s) is not known.

The decrease in ATP levels after hemorrhage was caused at least in part by decreases in the enzymatic activity and protein expression of PDH, an enzyme that catalyzes the oxidative decarboxylation of pyruvate to generate acetyl-CoA, thereby linking glycolysis to the tricarboxylic acid cycle with respect to substrate. These hemorrhage-induced decreases are not likely related to the increase in caspase-3 because *iNOS* gene-transfected cells exhibited the increased caspase-3 activity and protein level without altering the levels of PDH and ATP (J. G. Kiang, unpublished data). However, the possibility that other caspases are involved in PDH metabolism cannot be ruled out. Furthermore, whether enzymes other than PDH are altered by hemorrhage remains to be elucidated. In this study, we found that GA treatment prevented the hemorrhage-induced decrease in PDH enzymatic activity and its subsequent decrease in ATP levels. Kline et al. (18) reported that increased ATP after activation of PDH improves heart function and metabolism after hemorrhagic shock. Therefore, this GA-mediated inhibition of the PDH activity reduction and ATP loss can be relevant in preventing MOD and MOF after hemorrhage. This was further confirmed by the observation of GA inhibition on mucosal injury of the hemorrhaged jejunum (Fig. 4, *B* vs. *D*). The view is reinforced by the following facts: *1*) GA induces HSP70i overexpression, which confers cytoprotection against hemorrhagic injury (13, 14, 17, 25); *2*) GA inhibits KLF6 expression that is activated by hemorrhage (13, 14) or wound repair (27); *3*) GA inhibits hemorrhage-induced iNOS overexpression, which diminishes iNOS-induced cell injury (9, 12–15, 25); *4*) GA treatment effectively decreases the hemorrhage-induced increase in apoptosis (14); and *5*) GA increases ATP levels (Fig. 11). Therefore, it is reasonable to surmise that GA has potential therapeutic effects and that it can be used to limit the acute and delayed injury resulted from hemorrhage.

We propose that the GA-induced inhibition of hemorrhage-induced ATP loss is in part mediated by its induction of HSP70i because *1*) HSP70 forced overexpression enables the increases in PDH enzymatic activity, its protein expression, and ATP levels; *2*) HSP70 siRNA treatment decreases PDH enzymatic activity, its protein expression, and ATP levels; and *3*) HSP70 forms complex with PDH in both mouse jejunum tissues and GA-treated cultured cells, which may preserve the PDH activity and its integrity. On the other hand, GA directly upregulates PDH protein, which may also contribute to the reduction of the ATP loss and mucosal injury induced by hemorrhage.

The GA-induced increase in ATP is external Na^+ dependent and influenced by external K^+. This observation is consistent with findings reported by Portelli (26), which indicate that Ca^{2+} and Na^+ favor the breaking of the high-energy bond of the ATP molecule, whereas K^+ and Mg^{2+} help rebuild it. Therefore, the absence of extracellular Na^+ and presence of additional extracellular K^+ do not favor ATP generation. Increases in extracellular K^+ may also increase the activity of Na^+-K^+-ATPase and thereby deplete intracellular ATP levels.

Figure 12 presents a model for the interaction between hemorrhage-induced changes, depicting points where GA might block these changes. On the basis of our data and those from other laboratories (30), hemorrhage decreases PDH enzymatic activity and its protein levels, which results in decreased intracellular ATP. Low ATP levels cause mitochondria disruption. Because apoptosis requires energy, if the levels of ATP remain at levels >15% of baseline, then apoptosis ensues.

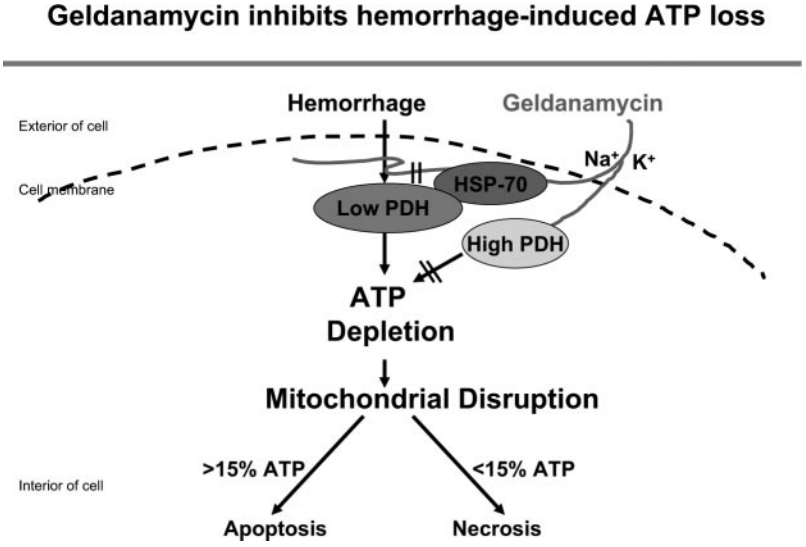

Fig. 12. Schematic representation of the model for ATP after hemorrhage and the points where GA might block the changes. Hemorrhage decreases PDH activity, which leads to low ATP levels. Low ATP levels cause mitochondrial disruption, which results in either apoptosis or necrosis depending on the level of ATP left in the cell (4, 19–21, 31). GA increases HSP70i expression, which forms complexes with PDH and preserves both protein levels and activity. GA also increases PDH protein. The GA-induced ATP increase is regulated by external Na^+ and K^+.

If the ATP levels fall below 15% of baseline, then necrosis ensues (4, 19–21, 31). Our observations show that GA treatment blocks the hemorrhage-induced decrease in PDH and increases PDH protein. The GA-induced HSP70i overexpression forms a complex with PDH, leading to cytoprotection. As a result, subsequent events are also blocked. The GA-induced ATP increase is regulated by external Na^+ and K^+.

In summary, we are the first to show that hemorrhage reduces PDH activity and its protein. GA treatment increases PDH activity and its protein as well as HSP70i protein. The increase in HSP70 forms a complex with PDH, together with an increased PDH protein level, to cytoprotect against undesirable outcomes such as ATP loss. Our results, taken together with findings from other laboratories (22, 25), indicate that GA may be therapeutically useful before surgery or as an additive to resuscitation fluids to reduce hemorrhage-induced injury.

ACKNOWLEDGMENTS

Authors thank Dr. Michael Zidanic for the microscopic assistance and R. Lee Collins for the graphic editing.

GRANTS

This study was supported by Department of Defense Research Area Directorate II Science and Technology Objective R.

DISCLAIMER

The opinions or assertions contained herein are the private views of the authors and are not to be construed as official or reflecting the views of the United States Department of the Army, the Uniformed Services University of the Health Sciences, or the United States Department of Defense.

REFERENCES

1. **Baue AE, Durham R, and Faist E.** Systemic inflammatory response syndrome (MODS), multiple organ dysfunction syndrome (MODS), multiple organ failure (MOF): are we winning the battle? *Shock* 10: 79–89, 1998.
2. **Chang CG, Van Way CW III, Dhar A, Helling T Jr, and Hahn Y.** The use of insulin and glucose during resuscitation from hemorrhagic shock increases hepatic ATP. *J Surg* 92: 171–176, 2000.
3. **Chaudry IH, Planer GJ, Sayeed MM, and Baue AE.** ATP depletion and replenishment in hemorrhagic shock. *Surg Form* 24: 77–79, 1973.

3a. **Chiu CJ, McArdle AH, Brown R, Scott HJ, and Gurd FN.** Intestinal mucosal lesion in low-flow states: a morphological, hemodynamic and metabolic reappraisal. *Arch Surg* 101: 478–483, 1970.

4. **Comelli M, Di Pancrazio F, and Mavelli I.** Apoptosis is induced by decline of mitochondrial ATP synthesis in erythroleukemia cells. *Free Radic Biol Med* 34: 1190–1199, 2003.
5. **Ding XZ, Tsokos GC, Smallridge RC, and Kiang JG.** Heat shock gene-expression in HSP70 and HSF1 gene-transfected human epidermoid A-431 cells. *Mol Cell Biochem* 167: 145–152, 1997.
6. **Du J, Wang X, Miereles C, Bailey JL, Debigare R, Zheng B, Price SR, and Mitch WE.** Activation of caspase-3 is an initial step triggering accelerated muscle proteolysis in catabolic conditions. *J Clin Invest* 113: 115–123, 2004.
7. **Fink MP.** Ethyl pyruvate: a novel treatment for sepsis and shock. *Minerva Anestesiol* 70: 365–371, 2004.
8. **Ghosh DK, Rashid MB, Crane B, Taskar V, Mast M, Misukonis MA, Weinberg JB, and Eissa NT.** Characterization of key residues in the subdomain encoded by exon 8 and 9 of human inducible nitric oxide synthase: a critical role for Asp-280 in substrate binding and subunit interactions. *Proc Natl Acad Sci USA* 98: 10392–10397, 2001.
9. **Hierholzer C, Harbrecht B, Menezes JM, Kane J, MacMicking J, and Nathan CF.** Essential role of induced nitric oxide in the initiation of the inflammatory responses after hemorrhagic shock. *J Exp Med* 187: 917–928, 1998.
10. **Hunt C and Morimoto RI.** Conserved features of eukaryotic hsp70 genes revealed by comparison with the nucleotide sequence of human hsp70. *Proc Natl Acad Sci USA* 82: 6455–6459, 1985.
11. **Kanematsu T, Higashi H, Takenaka K, Matsumata T, Maehara Y, and Sugimachi K.** Bioenergy status of human liver during and after warm ischemia. *Hepatogastroenterology* 37, *Suppl* 2: 160–162, 1990.
12. **Kiang JG.** Inducible heat shock protein 70 kD and inducible nitric oxide synthase in hemorrhage/resuscitation-induced injury. *Cell Res* 14: 450–459, 2004.
13. **Kiang JG, Bowman PD, Wu BW, Hampton N, Kiang AG, Zhao B, Juang YT, Atkins JL, and Tsokos GC.** Geldanamycin treatment inhibits hemorrhage-induced increases in KLF6 and iNOS expression in unresuscitated mouse organs: role of inducible HSP70. *J Appl Physiol* 97: 564–569, 2004.
14. **Kiang JG, Bowman PD, Wu BW, Hampton N, Kiang AG, Zhao B, Juang YT, Atkins JL, and Tsokos GC.** Geldanamycin inhibits hemorrhage-induced increases in caspase-3 activity, KLF6 and iNOS expression in unsuscitated organs of mice: role of inducible HSP70. *FASEB J* 18: A220–A221, 2004.
15. **Kiang JG, Lu X, Tabaku LS, Bentley TB, Atkins JL, and Tsokos GC.** Resuscitation with lactated Ringer solution limits the expression of molecular events associated with lung injury after hemorrhage. *J Appl Physiol* 98: 550–556, 2005.
16. **Kiang JG, McKinney LC, and Gallin EK.** Heat induces an intracellular acidification in human A-431 cells: role of Na^+/H^+ exchanger and metabolism. *Am J Physiol Cell Physiol* 259: C727–C737, 1990.
17. **Kiang JG, Warke VG, and Tsokos GC.** NaCN-induced chemical hypoxia is associated with altered gene expression. *Mol Cell Biochem* 245: 211–216, 2003.
18. **Kline JA, Maiorano PC, Schroeder JD, Grattan RM, Vary TC, and Watts JA.** Activation of pyruvate dehydrogenase improves heart function and metabolism after hemorrhagic shock. *J Mol Cell Cardiol* 29: 2465–2474, 1997.
19. **Leist M, Single B, and Castoldi AF.** Intracellular adenosine triphosphate (ATP) concentration: a switch in the decision between apoptosis and necrosis. *J Exp Med* 185: 1481–1486, 1997.
20. **Lemasters JJ.** V. Necrapoptosis and the mitochondrial permeability transition: shared pathways for necrosis and apoptosis. *Am J Physiol Gastrointest Liver Physiol* 276: G1–G6, 1999.
21. **Liberthal W, Menza SA, and Levine JS.** Graded ATP depletion can cause necrosis or apoptosis of cultured mouse proximal tubular cells. *Am J Physiol Renal Physiol* 274: F314–F327, 1998.
22. **Mabjeesh NJ, Post DE, Willard MT, Kaur B, Van Meir EG, Simons JW, and Zhong H.** Geldanamycin induces degradation of hypoxia-inducible factor 1α protein via the proteosome pathway in prostate cancer cells. *Cancer Res* 62: 2478–2482, 2002.
23. **Nalos M, Asfar P, Ichai C, Radermacher P, and Leverve XM.** Adenosine trisphosphate-magnesium chloride: relevance for intensive care. *Intensive Care Med* 29: 10–18, 2003.
24. **Paxian M, Bauer I, Rensing H, Jaeschke H, Mautes AE, Kolb SA, Wolf B, Stockhausen A, Jeblick S, and Bauer M.** Recovery of hepatocellular ATP and "pericentral apoptosis" after hemorrhage and resuscitation. *FASEB J* 17: 993–1002, 2003.
25. **Pittet JF, Lu LN, Geiser T, Lee H, Matthay A, and Welch WJ.** Stress preconditioning attenuates oxidative injury to the alveolar epithelium of the lung following hemorrhage in rats. *J Physiol* 538: 583–597, 2001.
26. **Portelli C.** The role of the sodium, potassium, magnesium and calcium ions in the transfer of energy at the level of the ATP molecule. *Physiologie* 13: 315–319, 1976.
27. **Ratziu V, Lalazar A, Wong L, Dang Q, Collins C, Shaulian E, Jensen S, and Friedman SL.** Zf9, a Kruppel-like transcription factor up-regulated in vivo during early hepatic fibrosis. *Proc Natl Acad Sci USA* 95: 9500–9505, 1998.
28. **Song Y, Ao L, Raeburn CD, Calkins CM, Abraham E, Harken AH, and Meng X.** A low level of TNF-α mediates hemorrhage-induced acute lung injury via p55 TNF receptor. *Am J Physiol Lung Cell Mol Physiol* 281: L677–L684, 2001.
29. **Stryer L.** *Biochemistry*. San Francisco, CA: Freeman, 1980, p.257–276.
30. **Van Way CW III, Dhar A, Morrison DC, Longorio MA, and Maxfield DM.** Cellular energetics in hemorrhagic shock: restoring adenosine triphosphate to the cells. *J Trauma* 54, *Suppl*: S169–S176, 2003.
31. **Wiegele G, Brandis M, and Zimmerhackl LB.** Apoptosis and necrosis during ischemia in renal tubular cells (LLC-PK and MDCK). *Nephrol Dial Transplant* 13: 158–1165, 1998.